Zel'dovich amplification in a superconducting circuit

Maria Chiara Braidotti[1,*] , Andrea Vinante[2,3], Giulio Gasbarri[2], Daniele Faccio[1], Hendrik Ulbricht[2,*]
[1]*School of Physics and Astronomy, University of Glasgow, G12 8QQ, Glasgow, UK.*
[2]*Department of Physics and Astronomy, University of Southampton, SO17 1BJ, Southampton, UK.*
[3]*Istituto di Fotonica e Nanotecnologie - CNR and Fondazione Bruno Kessler, I-38123 Povo, Trento, Italy.*

Zel'dovich proposed that electromagnetic (EM) waves with angular momentum reflected from a rotating metallic, lossy cylinder will be amplified. However, we are still lacking a direct experimental EM-wave verification of this fifty-year old prediction due to the challenging conditions in which the phenomenon manifests itself: the mechanical rotation frequency of the cylinder must be comparable with the EM oscillation frequency. Here we propose an experimental approach that solves this issue and is predicted to lead to a measurable Zel'dovich amplication with existing superconducting circuit technology. We design a superconducting circuit with low frequency EM modes that couple through free-space to a magnetically levitated and spinning micro-sphere placed at the center of the circuit. We theoretically estimate the circuit EM mode gain and show that rotation of the micro-sphere can lead to experimentally observable amplification, thus paving the way for the first EM-field experimental demonstration of Zel'dovich amplification.

In 1971, Zel'dovich predicted the amplification of electromagnetic (EM) waves scattering off a spinning metallic cylinder [1, 2], showing that the rotational energy of a spinning body can be transferred to the EM modes if the body spins rapidly enough, i.e. when

$$\omega < q\Omega, \tag{1}$$

where Ω is the cylinder rotation frequency and ω and q are the frequency and the order of the angular momentum of the incident EM radiation.

The importance of this effect, aside from its own intrinsic interest, lies in the tight connection to other phenomena, from super-radiant scattering, i.e. amplification of waves from a rotating black hole as predicted by Penrose in 1969 [3] to Hawking radiation i.e. evaporation of energy from a static black hole due to the interaction with quantum fluctuations [4]. Whereas laboratory analogues for these latter effects have been shown [5–9], we are still lacking experimental verification of Zel'dovich's idea, as originally proposed with EM waves. This appears to be simply due to a technological difficulty in satisfying the condition in Eq. (1), which nevertheless forces one to go back to carefully re-examine the underlying physical principles in order to propose a feasible experimental realisation.

Beyond Zel'dovich's original proposal, Bekenstein suggested to confine the EM mode in a cavity surrounding the metallic cylinder [10] so as to resonantly increase the amplification effect. More recently Gooding et al. [11] proposed to impinge on the rotating disk from the direction of the rotation axis, therefore harnessing the geometrical advantage of the dragging forces due to the penetration depth of the field inside the spinning body, as also suggested for acoustic experiments [12, 13]. However, this proposal also remains challenging [11], requiring a macroscopic body to spin at tens of GHz.

In this paper we describe a method to perform the original Zel'dovich experiment aimed at observing amplification of EM waves from a conductive rotating body.

In more detail, we theoretically study the scattering from a rotating, levitated sphere of an EM mode that has angular momentum, i.e. in particular orbital angular momentum (OAM). We show analytically how the amount of gain measured in the reflected EM mode depends on the choice of the sphere material. We consider both a conductive non-magnetic particle and a non-conductive ferro-magnetic particle, showing that the predicted gain should be observable in a real experiment.

The proposed system consists of a levitated conductive micro-sphere stably spinning at frequency Ω and a rotating EM mode used to probe the Zel'dovich effect.

Our proposed experimental set-up is schematically shown in Fig. 1. The EM field is the EM mode of a superconducting circuit that is composed of 4 micro-coils of equal inductance L. These micro-coils are near-field coupled to the spinning, free-space (i.e. not in physical contact with the circuit) micro-sphere. The micro-coils are joined by transmission lines of equal length $\ell/4$ in a closed loop thus forming a closed circuit (see Fig. 1). The chosen geometry, and in particular the length of wire between each coil, is such that adjacent micro-coils are phase-shifted by $\pi/2$ allowing propagating and counter-propagating normal modes of EM frequency $\omega = ck_q$, where c is the speed of light in vacuum, $k_q = 2\pi q/\ell$, and non-zero OAM $q = 1$ inside the circuit.

The whole system is placed in a cryogenic vacuum chamber at pressures of $\sim 10^{-5}$ mbar to enable low temperature measurements at $T \sim 4.2$ K (liquid helium temperature) or less, needed for superconducting technology and to obtain high electrical conductivities.

The initial driving to set the sphere in rotation is performed by switching the coil to an external circuit (not shown in Fig. 1). This driving magnetic field is generated by 4 waveform-generators, each synchronised with a $\pi/2$ phase shift, thus following the procedure demonstrated in [14, 15]. The driving field oscillates at a frequency

ω_d and induces the micro-sphere to rotate at a frequency $\Omega \lesssim \omega_d$. Ω can also be tuned by changing the intensity of the driving field [14, 15]. The maximum spinning frequency achievable with such a technique is only limited by the centrifugal forces overcoming the material stress limit and increases for decreasing sphere radius. For example, MHz rotation rates have been achieved by Schuck et al. with metallic spheres with a diameter of 0.5 mm [15].

Once the sphere reaches the desired rotation frequency the driving circuit and function generators are electronically switched off and probing is performed using the closed superconducting circuit shown in Fig. 1. In a vacuum of $\sim 10^{-5}$ mbar, we estimate that the levitated sphere will spin freely for more than one hour [15–17] (See Supplementary Material [18]), thus providing time to perform measurements with the superconducting circuit EM modes, under the assumption that these are significantly weaker than the driving EM field.

Theoretical analysis of the proposed system. The probe EM field is generated by a sinusoidal current passing through the inductors. The current in the j-th lumped inductor, corresponding to a propagating mode in the superconducting circuit, can be expressed as:

$$I_j\left(t\right) = \bar{I} e^{i(k_q \xi_j - \omega t - \phi_0)}, \tag{2}$$

where $\xi_j = j\ell/4$ denotes the coordinate of the position of each coil along the line and $j = (0, 1, 2, 3)$. ϕ_0 is an initial random phase and $\bar{I}$ is the peak current flowing in the coils due to the propagating wave. The current flowing in the circuit can be measured by a SQUID, weakly coupled through a small inductance in series with the circuit (not shown in Fig. 1).

In the chosen configuration, the total probe magnetic field induced by the coils can be written by means of the Biot-Savart formula for a circular loop as [19]:

$$\boldsymbol{B_0} = 2\beta \bar{I} \boldsymbol{b_0}, \quad \beta = \frac{N\mu_0}{8\sqrt{2}} \frac{1}{R}, \tag{3}$$

where $\boldsymbol{b_0} = (1, i, 0)^T e^{i\omega t}$, R is the radius of the micro-sphere, N is the number of loops of each coil and the factor 2 accounts for the contribution of the two opposite-facing coils. We observe that $\boldsymbol{B_0}$ is complex. In Eq. (3), we chose an arrangement of 4 micro-coils with radius $2R$ placed at a distance $2R$ from the center of the sphere (see Fig. 1b). This geometrical configuration has been chosen to maximise the coupling between the sphere and the coils. These parameters are also compatible with current technology: superconducting Niobium planar coils with $R \sim 100$ μm and high N, i.e. $N \sim 40$, can be fabricated using standard lithographic techniques and are typically used as input coils in conventional SQUIDs [20].

For simplicity the magnetic flux density $\boldsymbol{B_0}$ produced by the coils is assumed to be uniform over the microsphere volume, and the factor β in Eq. (3) is obtained by neglecting the thickness of each inductor. Thicker coils can also be considered, replacing the parameter β by an effective β_{eff} averaged over different loop. However, planar coils, having a large turn density, are the best candidates for this experiment [21]. An example of planar coil that can be fabricated with existing technology showing β_{eff} close to β is reported in the SM [18]. We assume the spinning sphere axis is oriented along z, with the origin of the transverse (x, y) plane set in the center of the sphere (see Fig. 1b). In the reference frame co-rotating with the micro-sphere, the magnetic flux density can be written as $\boldsymbol{B_r} = 2\beta \bar{I} \boldsymbol{b_r}$ with $\boldsymbol{b_r} = (1, i, 0)^T e^{i\omega_r t}$ and where $\omega_r = \omega - \Omega$ is the frequency of the field in the co-rotating reference frame. From the definition of ω_r we can see that a negative co-rotating frequency will satisfy the Zel'dovich condition Eq. (1) for $q = 1$ that can be expressed as $\omega_r = \omega - \Omega < 0$: we will show that when $\omega_r < 0$, the effective dissipation becomes negative, implying a conversion of rotational mechanical energy into energy of the circuit electromagnetic mode.

The interaction between the magnetic probe field and the rotating sphere induces a magnetic dipole moment $\boldsymbol{m_0}$ on the sphere, which in the laboratory frame can be written as

$$\boldsymbol{m_0} = \chi \boldsymbol{B_0} = (\chi' + i\chi'')\boldsymbol{B_0}, \tag{4}$$

where $\chi(\omega_r)$ is the complex response function of the sphere to the presence of the field in the co-rotating reference frame. The two vectors $\boldsymbol{m_0}$ and $\boldsymbol{B_0}$ rotate at the same EM frequency ω with an angular phase lag $\theta(\omega_r)$ determined by the imaginary part of the response function $\chi''(\omega_r)$ (see Fig. 1b), which gives rise to dissipation. If the sphere is conductive and non-magnetic, χ depends on the electric conductivity $\sigma(\omega_r)$ whereas for a ferro-magnetic ($\sigma = 0$) sphere, χ is proportional to the complex relative permeability $\mu_r(\omega_r)$ (see details in the Supplementary Material [18]).

The EM power dissipated by the sphere can be calculated as:

$$W = \frac{1}{2} \Re\{-\boldsymbol{m_0} \frac{d\boldsymbol{B_0^*}}{dt}\} = 4\beta^2 \omega \chi''(\omega_r) I_0^2, \tag{5}$$

where the factor 1/2 accounts for the average over one cycle, $\Re\{\cdot\}$ is the real part of the quantity in bracket, while $\boldsymbol{B_0^*}$ denotes the complex conjugate of the field [22]. The susceptibility $\chi(\omega_r)$ is the Fourier transform of the real-valued linear response function $\chi(t)$, which implies that $\chi''(-\omega_r) = -\chi''(\omega_r)$ [23]. A direct and key consequence of this is that when the Zel'dovich condition Eq. (1) is fulfilled, the power dissipated by the sphere becomes negative, i.e. power is radiated from the sphere into the EM circuit, leading to EM amplification.

The EM amplification can also be viewed as a result of the vector $\boldsymbol{m_0}$ preceding the vector $\boldsymbol{B_0}$, when $\omega_r < 0$ (rather than following it as usually happens when $\omega_r > 0$), as seen in the change of sign of rotation of the vector $\boldsymbol{m_r}$ in the co-rotating frame. Under these

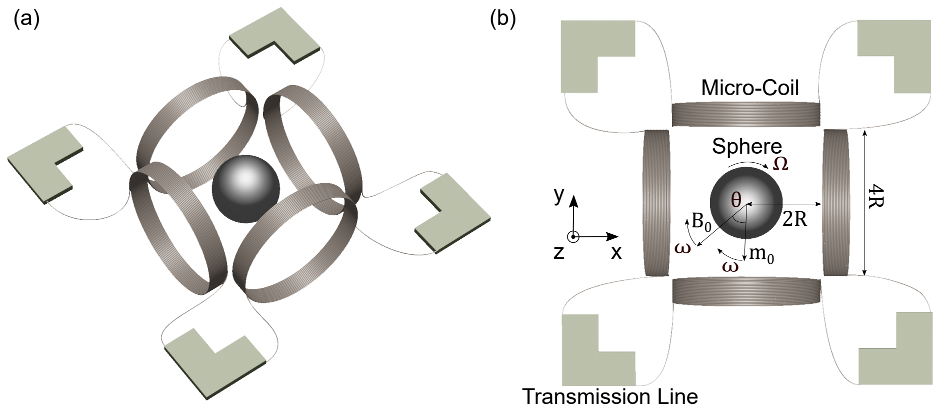

FIG. 1. (a) 3D Experimental set-up. (b) top view: the superconducting circuit is divided in 4 sections of length $\ell/4$, connected by 4 inductors with inductance L to form a closed ring configuration. The 4 coils have diameter equal to $4R$, where R is the radius of the central sphere, rotating at frequency Ω. The distance between each coil and the center of the sphere is $2R$. The arrows denote the magnetic field $\boldsymbol{B_0}$ generated by the 4 coils and the momentum $\boldsymbol{m_0}$ induced on the sphere. Both vectors rotate at frequency ω. θ is the angle between $\boldsymbol{B_0}$ and $\boldsymbol{m_0}$ and is related to the EM power dissipated in the sphere.

conditions the torque applied by the EM field, given by $\boldsymbol{T} = \Re\{\boldsymbol{m_0}\} \times \Re\{\boldsymbol{B_0}\} = -|\boldsymbol{B_0}||\boldsymbol{m_0}|sin(\theta)\hat{z}$, also becomes negative so that the EM field is extracting mechanical energy from the spinning sphere.

The total energy stored in the EM mode is $E = 1/2\,(L_0\ell + 4L)\,I_0^2$, where the first term is the energy stored in the transmission line and the second term is the energy stored in the 4 inductors. $L_0 = \sqrt{\varepsilon_r Z_0^2/c^2}$ is the transmission line inductance per unit length, where ε_r is the transmission line permittivity. The dissipation A, which is the key quantity we are interested in, can be finally expressed as the inverse of a quality factor, Q:

$$A = Q^{-1} = \frac{W}{\omega E} = \frac{8\beta^2\chi''}{(L_0\ell + 4L)}. \tag{6}$$

Under frequency inversion due to the Zel'dovich condition, χ'' and hence also A changes sign, so positive frequencies imply $A > 0$ while negative frequencies imply $A < 0$, i.e. gain.

We consider a rotating conductive micro-sphere with radius $R = 50$ μm and conductivity $\sigma \sim 5 \times 10^9$ Ohm^{-1}m^{-1}, i.e. similar to that of common copper (residual resistance ratio ≈ 100) at $T = 4 - 10$ K [24]. These parameters lead to rotational frequencies in the MHz range. This choice derives from a trade-off between conflicting requirements in the proposed experiment: a not too small sphere size to be compatible with existing fabrication and levitation technologies, and a high enough frequency ω to use transmission lines with realistic length. Figure 2 shows the predicted dissipation A induced by the micro-sphere obtained as a function of the EM frequency, ω, and rotation frequency, Ω. Figure 2 clearly shows a transition from absorption to amplification when ω approaches the sphere rotation frequency Ω, thus showing evidence of a relatively strong Zel'dovich amplification that should be readily observable. Indeed, for $\omega > \Omega$, $A > 0$, i.e. the particle absorbs the magnetic radiation impinging on it as expected. On the other hand, for $\omega < \Omega$, A becomes negative, and hence the $\boldsymbol{B}$ field is amplified when scattered from the rotating sphere.

Fixing a feasible micro-sphere rotation frequency at $\Omega/2\pi = 2.5$ MHz, we predict a maximum negative dissipation (i.e. gain) of $A_{max} \simeq -2 \times 10^{-3}$ (see Fig. 2b showing a line-out from Fig. 2a along the white dashed line at $\Omega/2\pi = 2.5$ MHz). We note that the chosen frequency is below the fundamental limit to the maximum rotation frequency $\Omega_{\rm max}$ that is determined by the sphere breaking apart. The breaking frequency scales with the inverse of radius and for $R = 50$ μm we estimate $\Omega_{\rm max}/2\pi \approx 3.5$ MHz, indicated in Fig. 2a by the dot-dashed black line. The red shaded area denotes the physically inaccessible region of frequencies due to the breaking of the micro-sphere [15]. The scaling of the dissipation A as function of R can be found in the SM [18].

Figure 2c shows the dissipation A trend for a fixed circuit frequency $\omega/2\pi = 2.5$ MHz as function of the micro-sphere rotation frequency $\Omega/2\pi$.

Proposed experiment design details. In an experiment, the EM mode frequency of 2.5 MHz can be obtained with a transmission line (see Fig. 1) formed by a compact coplanar waveguide of total length $\ell = |2\pi c/(\omega\sqrt{\varepsilon_r})| \sim 74.8$ m, where c is the speed of light and $\varepsilon_r = 6.38$ for a silicon substrate. Each section of the circuit will need to be $\ell/4 = 18.7$ m long. 2-m long coplanar waveguides are routinely fabricated in superconducting Kinetic Inductance Traveling Amplifiers (KIT), on a typical chip area of 20×20 mm^2 [25, 26]. These circuits are typically based on a double spiral geometry with constant pitch p, for which the area S is approximately proportional to the spiral length d by

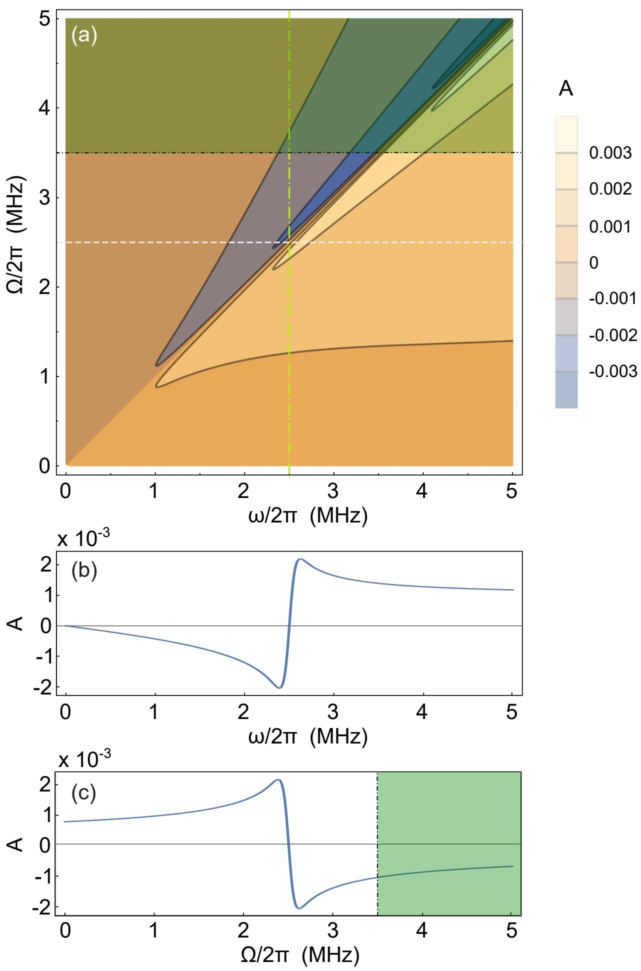

FIG. 2. (a) Rotational dissipation A as function of the magnetic field and sphere frequencies $\omega/2\pi$ and $\Omega/2\pi$. (b) A vs $\omega/2\pi$ for a fixed sphere rotation frequency $\Omega/2\pi = 2.5$ MHz of the particle (white dashed line in Fig. 2a). (c) A vs $\Omega/2\pi$, fixing the field frequency $\omega/2\pi = 2.5$ MHz of the particle (green dot-dashed line in Fig. 2a). In panel (a) and (c) the dot-dashed black line denotes the micro-sphere maximum rotations frequency $\Omega_{max}/2\pi = 3.5$ MHz and the green shaded area denotes the inaccessible region of frequencies. The parameters used are: $\sigma = 5 \times 10^9$ Ohm^{-1} m^{-1}, $\mu_r = 1$, $N = 40$, $Z_0 = 50$ Ohm, $R = 50$ μm, $\ell = 74.8$ m, $\epsilon_r = 6.34$.

the relation $S = pd$. By scaling existing spiral design [26] a length of 18 m corresponds to a maximum radius of 3.8 cm. This is well within the current industrial standard for silicon wafers. This size is also compatible with standard commercial cryostats [27].

In order to evaluate the experimental observability of the amplification, we need to also compare A_{max} with all the other sources of dissipation, A_0, in the electromagnetic modes, such as circuit losses. Meander-like superconductive coplanar waveguides (i.e. the KITs proposed above) or micro-coaxial niobium cables can be assumed to have $A_0^{wg} \sim 10^{-5}$ [28–30]. Furthermore, micro-coils in LC circuits show an intrinsic dissipation upper limit of $A_0^{coils} \sim 10^{-4}$ [31]. These contributions are all more than one order of magnitude smaller than the gain predicted in Fig. 2 and are not expected to therefore contribute appreciably.

Other materials for the sphere may also be considered. For example, in the Supplementary Material [18] we show that a smaller amplification, of the order of 10^{-5}, can be achieved by magnetic particles of ferrite with moderate permeability $\mu_r \approx 900$ [32]. A similar analysis for the case of simultaneously conductive and magnetic materials (data not shown) leads to lower gain factors in comparison to the purely conductive case presented here. In the dielectric case, reported in the Supplementary Material [18], A is 5 orders of magnitude smaller due to limitations in the electric field amplitude that can be generated by capacitors (which now substitute the magnetic field and inductors, respectively).

We further observe that the particle does not need to be fully metallic. It can be a composite with a ferromagnetic core which allows an easier levitation [33] and a highly conductive coating such that the coating thickness is comparable to the penetration depth of the EM field (see Ref. [18]).

Conclusions. We propose a superconducting circuit combined with a free-space, rotating sphere that is coupled to the circuit: this provides efficient EM-sphere coupling at low EM frequencies which in turn allow to access experimentally feasible rotational frequencies for the sphere, as required by the Zel'dovich condition.

Our calculations show that the proposed set-up exhibits measurable amplification of EM waves from mechanical rotation of both metallic and magnetic particles. It is worth noting that if GHz rotation frequencies could be reached with a similar scheme, then the circuit can be cooled to milli-kelvin temperatures where the thermal population is negligible, i.e. $k_b T < \hbar\omega$, a condition which has enabled superconducting quantum electrodynamics (QED) [34] and the study of fundamental physical effects such as dynamical Casimir emission [35, 36]. GHz rotation frequencies have been obtained with optical trapping of sub-micron sized spheres [37, 38]. This would require to arrange 4 nano-coils at distance $\sim$ 100 nm from the particle, which is incompatible with a realistic trapping laser waist. Moreover, the combination of a high power laser beam with a milli-Kelvin environment would require careful control of heat dissipation aspects. However, if these technological issues can be solved, spontaneous Zel'dovich emission could then also be observed i.e. rotational generation of photons out of the quantum vacuum [1] in a superconducting QED experiment. In addition, the system proposed here relies on a new generation of superconducting circuits coupled to rapidly moving elements, thus allowing the study of further fundamental physics problems such as the detection of rotational quantum friction [39–41] and quantum vacuum friction [42].

Acknowledgments. DF and MCB acknowledge financial support from EPSRC (UK Grant No. EP/P006078/2) and the European Union's Horizon 2020 research and innovation programme under Grant Agreement No. 820392. HU, AV and GG acknowledge financial support from the EU H2020 FET project TEQ (Grant No. 766900) and the Leverhulme Trust (RPG-2016-046). AV thanks Iacopo Carusotto for helpful discussions.

---

* mariachiara.braidotti@glasgow.ac.uk, h.ulbricht@soton.ac.uk

[1] Y. B. Zel'Dovich. Generation of waves by a rotating body. *ZhETF Pisma Redaktsiiu*, 14:270, 1971.

[2] Y. B. Zel'Dovich. Amplification of cylindrical electromagnetic waves reflected from a rotating body. *Soviet Physics-JETP*, 35:1085–1087, 1972.

[3] R Penrose. Gravitational Collapse: The Role of General Relativity. *Rivista del Nuovo Cimento*, (Numero Speziale I):25, 1969.

[4] S. Hawking. Black hole explosions? *Nature*, 248:30–31, 1974.

[5] G. Rousseaux, C. Mathis, P. Maïssa, T. G. Philbin and U. Leonhardt. Observation of negative-frequency waves in a water tank: a classical analogue to the Hawking effect? *New J. Phys.*, 10:053015, 2008.

[6] T. Torres, S. Patrick, A. Coutant, M. Richartz, E. W. Tedford, and S. Weinfurtner. Rotational superradiant scattering in a vortex flow. *Nature Phys.*, 13:833–836, 2017.

[7] Silke Weinfurtner, Edmund W. Tedford, Matthew C. J. Penrice, William G. Unruh, and Gregory A. Lawrence. Measurement of stimulated Hawking emission in an analogue system. *Phys. Rev. Lett.*, 106:021302, Jan 2011.

[8] J. Steinhauer. Observation of quantum Hawking radiation and its entanglement in an analogue black hole. *Nature Phys.*, 12:959–965, 2016.

[9] J. R. M. de Nova, K. Golubkov, V. I. Kolobov, and J. Steinhauer. Observation of thermal hawking radiation and its temperature in an analogue black hole. *Nature*, 569:688–691, 2019.

[10] J. D. Bekenstein and M. Schiffer. The many faces of superradiance. *Phys. Rev. D.*, 58(6):064014, 1998.

[11] C. Gooding, S. Weinfurtner, and W. G. Unruh. Reinventing the Zel'dovich wheel. *arXiv:1907.08688*, 2019.

[12] D. Faccio and E. M. Wright. Superradiant amplification of acoustic beams via medium rotation. *Physical review letters*, 123(4):044301, 2019.

[13] C. Gooding, S. Weinfurtner, and W. G. Unruh. Superradiant scattering of orbital angular momentum beams. *arXiv:1809.08235*, 2018.

[14] T. Reichert, T. Nussbaumer, and J. W. Kolar. Complete analytical solution of electromagnetic field problem of high-speed spinning ball. *Journal of Applied Physics*, 112(10):104901, 2012.

[15] M. Schuck, D. Steinert, T. Nussbaumer, and J. W. Kolar. Ultrafast rotation of magnetically levitated macroscopic steel spheres. *Science advances*, 4(1):e1701519, 2018.

[16] D. H. Gabis, S. K. Loyalka, and T. S. Storvick. Measurements of the tangential momentum accommodation coefficient in the transition flow regime with a spinning rotor gauge. *J. Vac. Sci. Technol. A*, 14:2592–2598s, 1996.

[17] P.S.Epstein. On resistance experienced by spheres in their motion through gases. *Phys. Rev.*, 23:710, 1924.

[18] See Supplemental Material [url] for additional information on the penetration depth and the calculations of the dissipation A with a ferro-magnetic micro-sphere and a dielectric one, which includes Refs. [43–46].

[19] D.J. Griffiths. *Introduction to Electrodynamics (3rd ed.)*. Prentice Hall, 1998.

[20] J. Clarke and A. I. Braginski. *The SQUID Handbook*. Wiley-VCH Verlag GmbH and Co., 2004.

[21] M. Peruzzo, A. Trioni, F. Hassani, M. Zemlicka, and J. M. Fink. Surpassing the resistance quantum with a geometric superinductor. *arXiv:2007.01644v1*, 2020.

[22] L. D. Landau and E. M. Lifshitz. *Electrodynamics of contnuous media (2nd ed.)*. Pergamon Press, 1984.

[23] L. D. Landau and E. M. Lifshitz. *Statistical physics (3rd ed.)*. Pergamon Press, 1980.

[24] https://www.copper.org/resources/properties/cryogenic/.

[25] L. Ranzani, M. Bal, K. C. Fong, G. Ribeill, X. Wu, J. Long, H.-S. Ku, R. P. Erickson, D. Pappas, and T. A. Ohki. Kinetic inductance traveling-wave amplifiers for multiplexed qubit readout. *Appl. Phys. Lett.*, 113:242602, 2018.

[26] B. Ho Eom, P. Day, and H. LeDuc. A wideband, low-noise superconducting amplifier with high dynamic range. *Nature Phys.*, 8:623–627, 2012.

[27] https://schoonoverinc.com/vacuum-maintenance/laboratory-cryo-cooler/custom-chamber-cryocooler/.

[28] Aaron D O'Connell, M Ansmann, Radoslaw C Bialczak, Max Hofheinz, Nadav Katz, Erik Lucero, C McKenney, Matthew Neeley, Haohua Wang, Eva M Weig, et al. Microwave dielectric loss at single photon energies and millikelvin temperatures. *Applied Physics Letters*, 92(11):112903, 2008.

[29] J. Zmuidzinas. Superconducting microresonators: Physics and applications. *Annu. Rev. Condens. Matter Phys.*, 3(1):169–214, 2012.

[30] P. Kurpiers, T. Walter, P. Magnard, Y. Salathe, and A. Wallraff. Characterizing the attenuation of coaxial and rectangular microwave-frequency waveguides at cryogenic temperatures. *EPJ Quantum Technology*, 4(1):1–15, 2017.

[31] L. Gottardi, J. van der Kuur, M. Bruijn, A. van der Linden, M. Kiviranta, H. Akamatsu, R. den Hartog, and K. Ravensberg. Intrinsic losses and noise of high-q lithographic mhz lc resonators for frequency division multiplexing. *Journal of Low Temperature Physics*, 194:370–376, 2019.

[32] https://www.pptechnology.com/.

[33] A. Vinante, P. Falferi, G. Gasbarri, A. Setter, C. Timberlake, and Ulbricht H. Ultralow mechanical damping with meissner-levitated ferromagnetic microparticles. *Phys. Rev. Applied*, 13:064027, 2020.

[34] C. M. Wilson, G. Johansson, A. Pourkabirian, M. Simoen, J. R. Johansson, T. Duty, F. Nori, and P. Delsing. Microwave photonics with superconducting quantum circuits. *Nature*, 470:376–379, 2011.

[35] C. M. Wilsonand G. Johansson, A. Pourkabirian, M. Simoen, J. R. Johansson, T. Duty, F. Nori, and P. Delsing. Observation of the dynamical casimir effect

in a superconducting circuit. *Nature*, 479:376–379, 2011.

[36] Pasi Lähteenmäki, G. S. Paraoanu, Juha Hassel, and Pertti J. Hakonen. Dynamical casimir effect in a josephson metamaterial. *PNAS*, 110:4234–4238, 2013.

[37] René Reimann, Michael Doderer, Erik Hebestreit, Rozenn Diehl, Martin Frimmer, Dominik Windey, Felix Tebbenjohanns, and Lukas Novotny. Ghz rotation of an optically trapped nanoparticle in vacuum. *Phys. Rev. Lett.*, 121:033602, 2018.

[38] Jonghoon Ahn, Zhujing Xu, Jaehoon Bang, Yu-Hao Deng, Thai M. Hoang, Qinkai Han, Ren-Min Ma, and Tongcang Li. Optically levitated nanodumbbell torsion balance and ghz nanomechanical rotor. *Phys. Rev. Lett.*, 121:033603, 2018.

[39] R. Zhao, A. Manjavacas, F. J. García de Abajo, and J. B. Pendry. Rotational quantum friction. *Phys. Rev. Lett.*, 109:123604, 2012.

[40] A. Manjavacas and F. J. García de Abajo. Thermal and vacuum friction acting on rotating particles. *Phys. Rev. A*, 82:063827, 2010.

[41] A. Manjavacas and F. J. García de Abajo. Spontaneous emission by rotating objects: A scattering approach. *Phys. Rev. Lett.*, 108:230403, 2012.

[42] P. C. W. Davies. Quantum vacuum friction. *J. Opt. B: Quantum Semiclass. Opt.*, 7:S40–S46, 2005.

[43] R. P. Feynman, R. B. Leighton, and M. Sands. *The Feynman Lectures on Physics.* Addison–Wesley, 2005.

[44] https://www.mag-inc.com/.

[45] J. P. Cosier and R. F. Pearson. Low-temperature permeability measurements on ferrites. *Br. J. Appl. Phys.*, (18):615, 1967.

[46] N. S. Midi, K. Sasaki, R. Ohyama, and N. Shinyashiki. Broadband complex dielectric constants of water and sodium chloride aqueous solutions with different dc conductivities. *IEEJ Trans.*, 9:8–12, 2014.